BMC Pharmacology and Toxicology

RESEARCH Open Access

Potential cardioprotective effect of paroxetine against ventricular remodeling in an animal model of myocardial infarction: a comparative study

Asma S. Alonazi[1*], Sara Almodawah[2], Rana Aldigi[2], Anfal Bin Dayel[1], Maha Alamin[1], Ahmad R. Almotairi[3], Maha F. El-Tohamy[4], Hana Alharbi[1], Rehab Ali[1], Tahani K. Alshammari[1] and Nouf M. Alrasheed[1]

Abstract

Background Post-myocardial infarction (MI) remodeling involves various structural and functional changes, such as inflammation and fibrosis. Upregulation of G protein-coupled receptor kinase 2 (GRK2) is linked to the progression of cardiovascular diseases, including myocardial infarction. The inhibitory effects of paroxetine on GRK2 are recognized, yet its protective effect on post-MI remodeling has not been elucidated. Here, we investigated the cardioprotective effect of paroxetine in an animal model of MI, focusing on post-MI cardiac remodeling and comparing its effect to a β-blocker and an angiotensin receptor antagonist.

Methods Albino Wistar rats were divided into five groups (control; untreated MI; and MI pre-treated with either paroxetine, metoprolol, or irbesartan). MI was induced using isoproterenol (100 $mg.kg^{-1}$) on days 16 and 17. Cardioprotective effects were determined by assessing markers of cardiac injury, histopathology, inflammation, oxidative stress, and fibrosis. Statistical analysis performed using a one-way analysis of variance, followed by an appropriate post hoc test, the differences between the groups were considered significant when the ($P < 0.05$).

Results Paroxetine significantly attenuated cardiac injury biomarkers including serum Tn-I and CK-MB levels. In terms of cardiac remodeling, paroxetine significantly reduced the relative HW/BW index and the plasms FGF23 level. Furthermore, it modulated markers of fibrosis, inflammation, and oxidative stress.

Conclusion The current findings suggest that pre-treatment with paroxetine may exert a beneficial effect that protects against post-MI remodeling, including modulating fibrotic, inflammatory, and angiogenesis-related factors. Therefore, the current findings show the promising role of paroxetine as a cardioprotective that attenuates post-MI remodeling processes.

Keywords Myocardial infarction, Ventricular remodeling, GRK2, Paroxetine

*Correspondence:
Asma S. Alonazi
aaloneazi@ksu.edu.sa
[1]Department of Pharmacology and Toxicology, College of Pharmacy, King Saud University, Riyadh, Saudi Arabia
[2]College of Pharmacy, King Saud University, Riyadh, Saudi Arabia
[3]Department of Pathology, College of Medicine, King Saud University, Riyadh, Saudi Arabia
[4]Department of Chemistry, College of Science, King Saud University, Riyadh, Saudi Arabia

© The Author(s) 2024. **Open Access** This article is licensed under a Creative Commons Attribution-NonCommercial-NoDerivatives 4.0 International License, which permits any non-commercial use, sharing, distribution and reproduction in any medium or format, as long as you give appropriate credit to the original author(s) and the source, provide a link to the Creative Commons licence, and indicate if you modified the licensed material. You do not have permission under this licence to share adapted material derived from this article or parts of it. The images or other third party material in this article are included in the article's Creative Commons licence, unless indicated otherwise in a credit line to the material. If material is not included in the article's Creative Commons licence and your intended use is not permitted by statutory regulation or exceeds the permitted use, you will need to obtain permission directly from the copyright holder. To view a copy of this licence, visit http://creativecommons.org/licenses/by-nc-nd/4.0/.

Introduction

Cardiovascular diseases (CVDs) are a major global health concern, accounting for 17.8 million annual deaths [1]. Over half of CVD-related deaths are attributable to ischemic heart diseases such as myocardial infarction (MI) [2]. The burden of the mortality and morbidity of CVDs significantly impacts healthcare systems and patients' quality of life [3]. MI is defined as irreversible cardiomyocyte damage or loss of myocardial tissue resulting from acute obstruction of a coronary artery, resulting in a severe reduction in coronary artery blood flow to the cardiomyocytes [4]. MI can be diagnosed based on electrocardiography (ECG) and the presence of circulating cardiac injury biomarkers such as creatine kinase, cardiac troponins, and lactate dehydrogenase (LDH). These biomarkers serve as supportive evidence for the diagnosis of MI [5]. Following MI, the myocardium undergoes a complex process of structural and functional alterations consisting of three main phases—the inflammatory phase, proliferative/reparative phase, and maturation phase—collectively defined as cardiac remodeling [6].

The inflammatory phase is accompanied by the activation of chemokine and cytokine cascades such as TNF-α, IL-1, IL-6, and IL-18, which leads to local infiltration of leukocytes such as macrophages, monocytes, and neutrophils into the infarct area. The proliferative/reparative phase comes next. It is characterized by producing profibrotic and inflammatory cytokines, including TGF-β and IL-10, that promote tissue repair and decrease inflammation [6, 7]. After the inflammatory phase, the proliferative/reparative phase begins. Myofibroblasts and vascular cells are primarily recruited and activated, while proinflammatory mediators are inhibited by the production of cytokines and growth factors [8]. Vascular endothelial growth factor (VEGF), a growth factor with significant pro-angiogenic activity, is upregulated during the proliferative/reparative phase post-MI. It promotes the formation of new blood vessels to supply the infarcted cardiomyocytes with oxygenated blood, compensating for the hypoxia [9]. The final phase is the maturation phase, where the scar formed in the infarcted area matures and becomes more stable by producing extracellular matrix proteins such as collagen, resulting in fibrosis [8]. Although early cardiac remodeling can initially restore heart function by maintaining blood flow, excess or prolonged remodeling might have detrimental consequences, such as ventricular dilation, ventricular hypertrophy, and heart failure [10].

Recent studies reported that CVDs have been associated with changes in the expression and activity of molecules that regulate G protein-coupled receptors (GPCRs), particularly G protein-coupled receptor kinase 2 (GRK2) [11]. G protein-coupled receptor kinase 2 (GRK2) is a serine/threonine kinase that plays a key role in regulating the function of GPCRs, including β-adrenergic receptors (β-ARs), that regulate various cellular and physiological responses, such as cardiac contractility, growth, and metabolism [12, 13]. GRK2 was previously shown to be a key regulator involved in intracellular β-AR signaling. Furthermore, GRK2 was determined to be the main kinase involved in cardiac β-AR dysregulation. GRK2 upregulation decreases β-AR responsiveness via chronic receptor desensitization and downregulation. It is initially triggered by SNS overstimulation, which causes diminished sensitivity and reduces the number of functional receptors, contributing to impaired β-adrenergic signaling and potential cardiac dysfunction [14, 15]. Recent evidence showed that GRK2 is upregulated in cardiovascular diseases such as heart failure, cardiac hypertrophy, and hypertension, which have been linked to elevated GRK2 expression and activity through several processes that are connected to its multifunctional activities. Therefore, GRK2 could be explored as a potential target for various cardiovascular diseases, including myocardial infarction, heart failure, and hypertension [16, 17].

Paroxetine belongs to a class of medications called selective serotonin reuptake inhibitors (SSRIs), which are used clinically in the treatment of depression and anxiety disorders [18]. Recent evidence showed that paroxetine exerts an inhibitory effect on GRK2, as it enhanced β-AR-dependent cardiomyocyte responses in both in vitro and in vivo studies [19, 20]. In 2015, Schumacher S. M et al. investigated the effect of paroxetine in a post-MI mouse model. They showed that paroxetine can significantly improve left ventricular structure and function and can diminish adrenergic overstimulation [21]. The published reports suggest that paroxetine might have a cardioprotective effect [22–24]. However, its protective effect on MI-induced cardiac remodeling has not been elucidated.

Multiple pharmaceutical approaches have been shown to be effective in reducing MI outcomes, such as targeting the β-adrenergic system. In clinical settings, a two-year follow-up study in Korean MI patients showed that β-blockers reduce risks by almost 40% [25]. Another strategy targets the angiotensin II type 1 (AT-1) receptor [26]. In spite of pharmacological advances, the rate of mortality associated with MI outcomes is elevated. The need to understand the MI-related pathophysiological mechanisms and find an optimal therapeutic intervention is unmet [27]. Here, we aimed to investigate the cardioprotective effect of paroxetine, as a GRK2 inhibitor, on the progression of MI-associated remodeling, including inflammation, angiogenesis, oxidative stress, and fibrosis. Furthermore, this study compared its effects to those of a β-blocker and an AT1 receptor antagonist.

Materials and methods

Animals

Forty adult male albino Wistar rats were carefully obtained from The Animal Care Centre at the College of Pharmacy of King Saud University (KSU) in Riyadh, Saudi Arabia. These rats were maintained in controlled conditions with a temperature of 25±1 °C, a 12-hour light/dark cycle, and a humidity level of 60%. To ensure their well-being, they had access to tap water and consumed food ad libitum. This research followed the ethical guidelines set by the KSU Experimental Animals Ethics Committee, guaranteeing that the rats received ethical treatment throughout the study (Reference: KSU-SE-23-41 (16th May 2023)).

Induction of experimental myocardial infarction

After allowing the rats to acclimate to their environment for one week, they were divided into five groups (eight rats each) (Fig. 1). Experimental myocardial infarctions were induced in the rats using Isoproterenol (ISO) according to a previously published protocol [28]. ISO was dissolved in normal saline and injected into the rats (100 mg/kg) intraperitoneally (i.p.) on two consecutive days (days 16 and 17) at an interval of 24 h. The control animals received normal saline (0.9% NaCl), while the other rats were pre-treated as follows:

Group 1 (C): the normal control rats received normal saline throughout the experiment.

Group 2 (MI): These rats received normal saline for two weeks and then received ISO (100 mg/kg i.p.) [29] on two consecutive days (days 16 and 17).

Group 3 (P + MI): these rats were pre-treated with paroxetine (5 mg/kg/day) [30] for two weeks, and then received ISO (100 mg/kg i.p.) on two consecutive days (days 16 and 17).

Group 4 (M + MI): these rats were pre-treated with metoprolol (10 mg/kg/day) [31] for two weeks, and then received ISO (100 mg/kg i.p.) on two consecutive days (days 16 and 17).

Group 5 (R + MI): these rats were pre-treated with irbesartan (50 mg/kg/day) [32] for two weeks, and then received ISO (100 mg/kg i.p.) on two consecutive days (days 16 and 17).

On day 20, at the end of the experiment, after overnight fasting, all rats were weighed and euthanized using carbon dioxide gas, and we verified their death by the absence of reflexes. Trunk blood samples were collected for biochemical analysis. The heart tissue was excised, weighed to obtain the heart weight to body weight ratio, quickly frozen in liquid nitrogen, and stored at -80 °C for the required analysis.

Evaluating heart weight/body weight ratio (HW/BW)

The HW/BW ratio was assessed as an index of the development of cardiac structural remodeling. Once the heart tissues were isolated, they were washed with normal

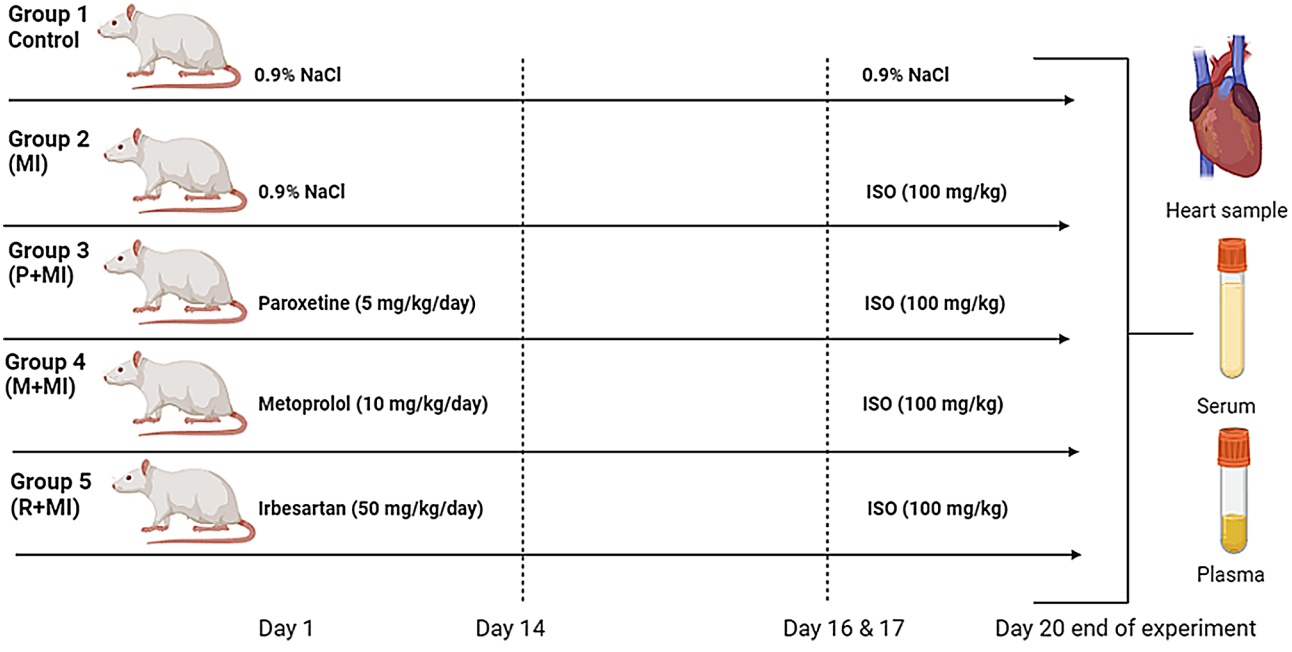

Fig. 1 Schematic of the experimental design

saline and weighed. The HW/BW ratio was then determined by dividing the heart weight (mg) by the final body weight (g) [33].

Examination of myocardial infarction biomarkers

To confirm MI induction, cardiac injury biomarkers were evaluated. The serum levels of cardiac injury biomarkers, including troponin 1 (Tn-I), creatine kinase myocardial band (CK-MB), and lactate dehydrogenase (LDH), were investigated using either an enzyme-linked immunosorbent assay (ELISA) or a colorimetric method according to the manufacturer's instructions. Briefly, serum Tn-I and CK-MB levels were examined using specific rat ELISA kits (Solarbio Life Sciences, Tongzhou District, Beijing, China) according to the manufacturer's instructions. The standard curve detected the cTnl and CK-MB concentrations in an unknown sample. Absorbance outcomes were read using a BioTek Microplate Reader (BioTek Instruments, Winooski, VT, USA) at a specified wavelength (λ=450 nm). The total levels of cTn-I (pg/ml) and CK-MB (ng/mL) were determined via linear regression analysis and compared with the known concentrations of standards. Furthermore, LDH was evaluated as a marker of ischemia. The serum LDH level was measured using a spectrophotometer activity assay kit (RANDOX Laboratories Ltd, Largy Rd, Gorthnagallon, Crumlin, UK). Briefly, serum samples from different rats in each group were used for the detection of LDH and to generate a standard curve according to the manufacturer's instructions. LDH was quantitatively determined in serum using a lactate-to-pyruvate kinetic method. The rate of NADH formation was indicated by an increase in absorbance at λ=340 nm and was directly proportional to the serum LDH activity.

Histopathological examination of the heart for cardiac remodeling

Cardiac samples were excised and fixed in 10% neutral buffered formalin (4% formaldehyde solution) for 24 h. Afterward, they underwent standard overnight processing, including dehydration, clearing, and infiltration, and were then embedded in paraffin. Thin Sect. (25 μm) were prepared from the samples and stained with hematoxylin and eosin (H&E) to investigate the morphological structure of the myocardium. Additionally, we utilized Masson's trichrome stain to identify heart fibrosis and the deposition of extracellular collagen. A Periodic Acid–Schiff stain (PAS) was also used to further investigate the changes in the heart sections. The sections from each group were examined under a light microscope (Olympus 51 microscope, Shinjuku, Tokyo, Japan) at 10X magnification (25 μm) by a certified surgical pathologist.

Evaluating plasma FGF23 as a marker of ventricular remodeling

The plasma levels of FGF23 were investigated using ELISA kits (Solarbio Life Sciences, Tongzhou District, Beijing, China) according to the manufacturer's instructions. Briefly, plasma samples from at least six rats per group were investigated. The standard curve was used to detect the FGF23 concentration in an unknown sample, and the absorbance results were read using a BioTek Microplate Reader (BioTek Instruments, Winooski, VT, USA) at a specified wavelength (λ=450 nm). The total plasma level of FGF23 (pg/ml) was determined via linear regression analysis and compared with the known concentrations of standards.

Evaluating hydroxyproline (HYP), TGF-β1, VEGF, and TNF-α in cardiac tissue

HYP is one of the main components of collagen. Thus, its content is an important index that reflects the degree of fibrosis and collagen accumulation in tissue [34]. An HYP activity assay kit (Solarbio Life Sciences, Tongzhou District, Beijing, China) was used to determine the HYP levels in the heart tissues according to the manufacturer's instructions. Briefly, equal amounts (about 0.25 g) of cardiac ventricle tissue were homogenized from different rats (n=6) in each group. The samples were hydrolyzed to produce free HYP, which was further oxidized by chloramine T. The oxidized product reacted with p-Dimethylaminobenzaldehyde to produce a red compound with a characteristic absorption peak at λ=560 nm. The colorimetric results were measured using a BioTek Microplate Reader. The total levels of HYP (μg/g) were determined via linear regression analysis and compared with the known concentrations of standards. On the other hand, the protein levels of TGF-β1, VEGF, and TNF-α were determined using ELISA kits (Solarbio life sciences, Tongzhou District, Beijing, China) according to the manufacturer's instructions. Heart tissue homogenates were used to examine the target proteins, and the absorbance was read for each target at a specified wavelength using a BioTek Microplate Reader.

Characterization of the activity of oxidative stress biomarkers

Glutathione Reductase (GSH) testing was performed according to a method previously reported by Moron et al. [35], with sight modification. Briefly, a heart tissue homogenate was mixed with 25% trichloroacetic acid and centrifuged for 10 min at 3000 rpm. Then, the supernatant was treated with Ellman's reagent. The resulting yellow product indicated the amount of GSH in the sample, as calculated using a spectrophotometer at 412 nm as units per mg of protein in the heart tissue.

Spectrophotometric measurements of SOD activity were carried out at 430 nm to ensure its creation. In addition, SOD activity was measured according to Delides et al. [36] to define the inhibition of this reaction using a nitro blue tetrazolium method. In this analysis, a single unit of SOD referred to the quantity of enzyme required to neutralize half of the superoxide radicals through dismutation, which was expressed as $U.mg^{-1}$ protein in the heart tissue. Lipid peroxidation (LPO) was quantified using the thiobarbituric acid (TBA)-reactive substances (TBARSs) assay described by Ohkawa et al. [37]. Treated heart tissue was centrifuged at 3,000 rpm for 10 min and sonicated to make a uniform solution. After centrifugation, the supernatant was collected, and about 500 µL was reacted with 1 mL of TBA and 2.5 ml of 20% trichloroacetic acid. This solution was incubated at 100 °C for 15 min in a water bath. It was then cooled and centrifuged for 2 min at 13,000×*g*. The resulting solution was separated, and the absorbance of the fluorescent adduct was recorded at 535 nm. The TBARSs were represented as minimum detectable activity (MDA) equivalents (units per mg of protein).

Immunoblotting

Heart ventricular tissue samples lysate was prepared according to the previously published protocol using RIPA buffer and protease inhibitors. Then, lysate samples (equal amount) were separated by sodium dodecyl sulfate-polyacrylamide gel electrophoresis (SDS-PAGE) at 120 V for 120 min. Then, transferred onto the PVDF membrane. After that, nonspecific binding sites were blocked by non-fat dry milk (5%) for one hour at room temperature. Blots were then incubated over night at 4°C with a primary antibody: anti-iNOS (1:1000), anti-GRK2 (1:1000), anti-β-actin (1:3000) and anti-GAPDH (1:3000) as a loading control. Next, the blots were incubated with secondary antibodies IRDye® 680RD Goat anti-Mouse IgG Secondary Antibody and IRDye® 800CW Goat anti-Rabbit IgG (1:15000). Band near-infrared fluorescent signals were visualized using the Odyssey® CLx Imaging System. Densitometrical analyses were performed for the detected protein bands using Image J (1.51) software.

Statistical analysis

Data were expressed as means ± SEM. To determine the differences between the groups, statistical analysis using a one-way analysis of variance (ANOVA), followed by Dunnett's post hoc test, was applied using GraphPad Prism 9. The differences between the groups were considered significant when the P-values were less than 0.05 ($P<0.05$).

Results

Paroxetine reduced ISO-induced cardiac injury, remodeling, and morphology

To interpret the effect of paroxetine in cardiac remodeling, the HW/BW ratio and cardiac injury biomarkers were evaluated. As expected, the HW/BW ratio was significantly enhanced in the infarcted hearts (Fig. 2A). Pre-treatment with paroxetine decreased the HW/BW ratio compared to the untreated group (5.431 ± 0.2103 vs. 4.461 ± 0.3056 mg/g, $P<0.01$). Cardiac injury biomarkers such as Troponin I, CK-MB, and LDH were also evaluated (Fig. 2). The cardiac serum LDH level showed a non-significant increase in the untreated infarction group, and pre-treatment with paroxetine reduced this level compared to the untreated group (Fig. 2B). Serum Troponin I was significantly increased in the infarcted hearts ($P<0.0001$), and pre-treatment with paroxetine decreased Troponin I compared to the untreated group (7.265 ± 0.2685 vs. 4.052 ± 0.1915 pg/ml, $P<0.0001$) (Fig. 2C). Similarly, serum CK-MB was significantly enhanced in the infarcted hearts ($P<0.0001$), and pre-treatment with paroxetine decreased CK-MB compared to the untreated infarction group (5.248 ± 0.7906 vs. 2.485 ± 0.03560 ng/ml, $P<0.0001$) (Fig. 2D). The effects of paroxetine on ISO-induced plasma FGF23 were also evaluated as markers of ventricular remodeling. As shown in Fig. 2F, the plasma level of FGF23 showed a non-significant increase in the infarcted hearts. Pre-treatment with paroxetine significantly decreased the FGF23 levels compared to the untreated infarction group (626.2 ± 79.32 vs. 310.3 ± 44.43 pg/ml, $P<0.05$) (Fig. 2E). The series of histological images presented in Fig. 2F demonstrates the diverse pathological changes observed in the rat cardiac muscle tissues across the different experimental groups. Following H&E staining, the normal control group illustrated a baseline healthy cardiac muscle architecture devoid of any significant pathological features. In contrast, the MI group showcased a compromised muscular structure with prominent infiltration by inflammatory cells, predominantly histiocytes and lymphocytes, coupled with noteworthy interstitial fibrosis. Interestingly, the P + MI and R + MI treatment groups exhibited reduced fibrosis and inflammatory cell presence, respectively. On the other hand, the M + MI treatment group demonstrated a varied pattern of small, localized areas of inflammatory infiltration and mild fibrosis, as further highlighted by the trichrome stains in Fig. 4C.

Effect of paroxetine GRK2 protein level

The level of GRK2 protein expression was noticeably elevated in myocardium tissues of MI-untreated group. As shown in Fig. 3, pre-treatment with paroxetine resulted

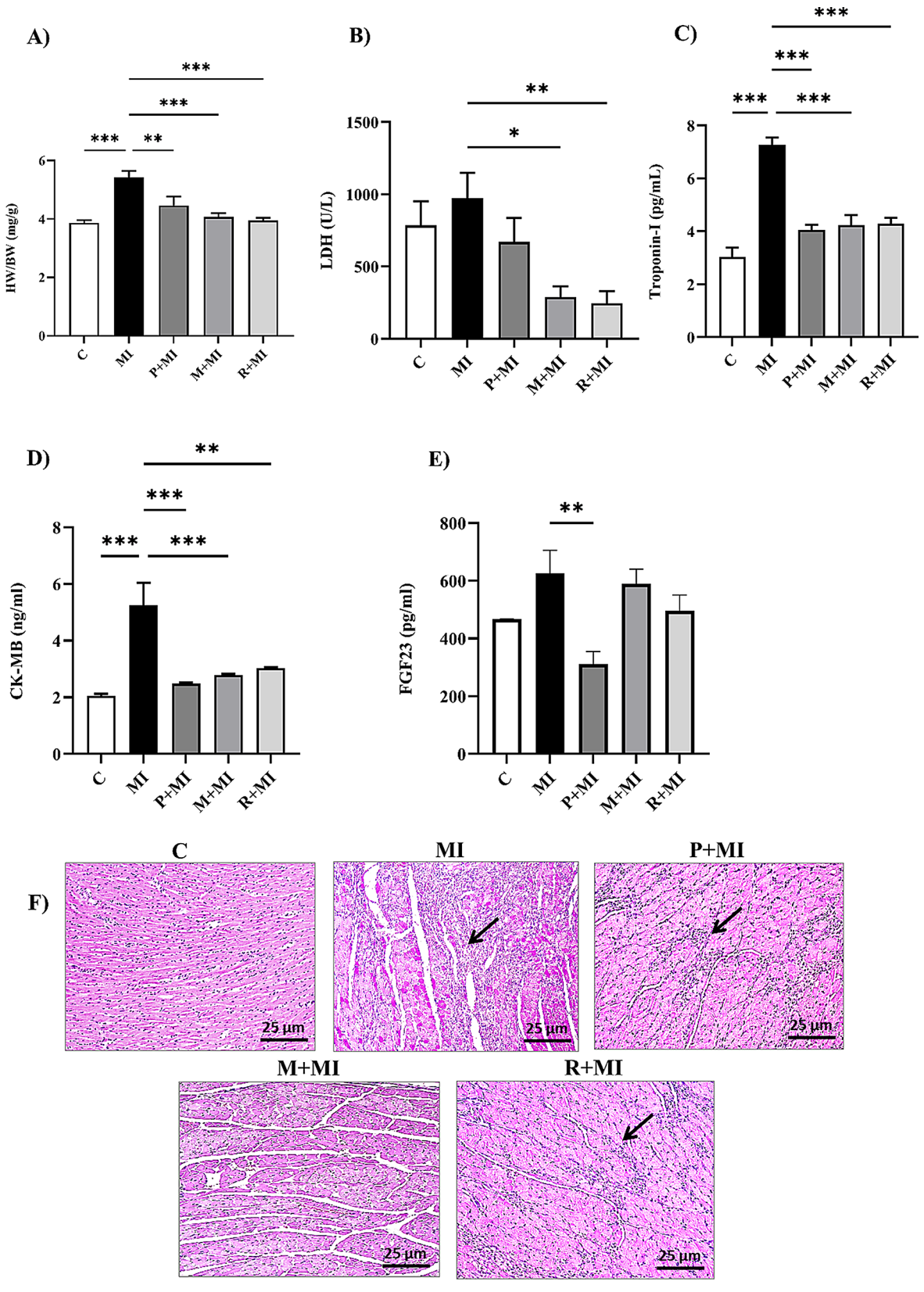

Fig. 2 (See legend on next page.)

(See figure on previous page.)

Fig. 2 Effects of paroxetine on markers of MI-induced cardiac injury. HW/BW ratio (**A**) as an indicator of cardiac hypertrophy. Serum levels of the cardiac injury biomarkers LDH (**B**), Tn-I (**C**), and CK-MB (**D**). Serum level of FGF23 as an indicator of cardiac remodeling (**E**). **F** H&E staining for cardiac muscle fascicles and fibers in the normal control group shows no inflammatory cell infiltration. The untreated (MI) group shows inflammatory cell infiltration, mainly histiocytes, with a few lymphocytes (black arrow) (20X power field). All data are expressed as means ± SEM. Differences between groups were determined using a one-way ANOVA followed by Dunnett's post hoc test. The total number of biological and technical replicates is 6 per group. Statistically significant changes compared to the untreated MI rats are indicated with * ($P<0.05$), ** ($P<0.01$), *** ($P<0.001$). *Abbreviations C* control, *MI* untreated myocardial infarction, *P + MI* myocardial infarction pre-treated with paroxetine, *M + MI* myocardial infarction pre-treated with metoprolol, *R + MI* myocardial infarction pre-treated with irbesartan

in a significant decrease in the GRK2 levels ($P<0.05$). Similarly, pre-treatment with metoprolol decreased the GRK2 levels significantly ($P<0.001$) compared to the untreated infarction group.

Effect of paroxetine on ISO-induced cardiac fibrosis

HYP was significantly enhanced in the infarcted hearts ($P<0.0001$), and pre-treatment with paroxetine decreased HYP compared to the untreated infarction group (4.857 ± 0.2142 vs. 3.858 ± 0.1971 mcg/g, $P<0.01$) (Fig. 4A). Similarly, TGF-β1 was significantly increased in the infarcted hearts ($P<0.0001$) and was decreased significantly by the paroxetine pre-treatment (104.7 ± 14.9 vs. 205.2 ± 13.9 pg/ml, $P<0.001$) compared to the untreated infarction group (Fig. 4B). Additionally, Fig. 4C further corroborates these observations with trichrome staining (MT), vividly illustrating the extent of fibrosis through differential staining patterns.

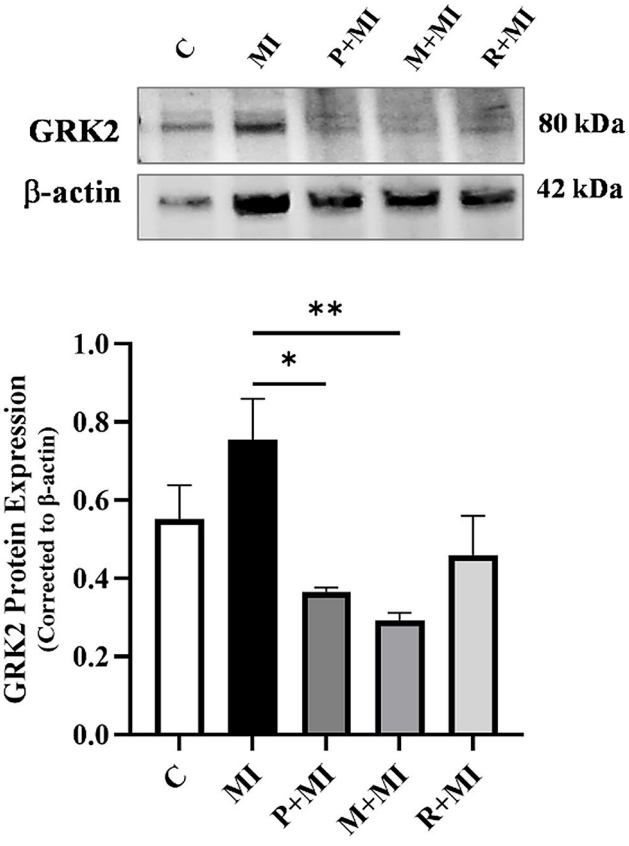

Fig. 3 Effect of paroxetine on GRK2 expression. Upper panel show a representative immunoblot of the GRK2 protein levels in the tissue homogenates of the left ventricle. Lower panel show the quantitative results of the immunoblot analysis. The GRK2 protein expression was normalized to β-actin and the band densities were quantified using ImageJ software. All data are expressed as means ± SEM ($n=4$). Differences between groups were determined using a one-way ANOVA followed by Dunnett's post hoc test. Statistically significant changes compared to the untreated MI rats are indicated with * ($P<0.05$), or *** ($P<0.001$). *Abbreviations C* control, *MI* untreated myocardial infarction, *P + MI* myocardial infarction pre-treated with paroxetine, *M + MI* myocardial infarction pre-treated with metoprolol, *R + MI* myocardial infarction pre-treated with irbesartan

Effect of paroxetine on ISO-induced inflammation

Tissue TNF-α levels and serum CRP were evaluated as indicators of inflammation. TNF-α was significantly increased in the infarcted hearts ($P<0.0001$). Pre-treatment with paroxetine significantly reduced the TNF-α levels compared to the untreated infarction group (503.4 ± 96.48 vs. 123.3 ± 31.16 pg/ml, $P<0.0001$) (Fig. 5A). Similarly, CRP was significantly enhanced in the MI group ($P<0.0001$). Pre-treatment with paroxetine significantly reduced the TNF-α levels compared to the untreated infarction group (45.71 ± 6.01 vs. 107.9 ± 10.65 pg/ml, $P<0.001$) (Fig. 5B). Additionally, Fig. 5C provides further insights with PAS staining, and PAS-positive macrophages are identified by black arrows. Notably, in all examined groups, no necrotic lesions, granulomas, eosinophilic infiltration, or multinucleated giant cells were detected, which would have indicated more severe or distinct chronic inflammatory states.

Effect of paroxetine on VEGF and iNOS expression

As shown in Fig. 6A, the VEGF levels were significantly enhanced in the infarcted hearts ($P<0.0001$). Pre-treatment with paroxetine decreased the VEGF levels significantly compared to the untreated infarction group (324.5 ± 46.92 vs. 115.1 ± 10.44 pg/ml, $P<0.0001$). Similarly, the iNOS protein levels were upregulated in the rats with MI. Pre-treatment with paroxetine resulted in a non-significant decrease in the iNOS levels, while pre-treatment with metoprolol decreased the iNOS levels significantly compared to the untreated infarction group (Fig. 6B).

Effects of paroxetine on oxidative stress biomarkers

Figure 7 shows the effects of paroxetine on the catalase, GSH, SOD, LPO, and total nitrate in the cardiac tissue.

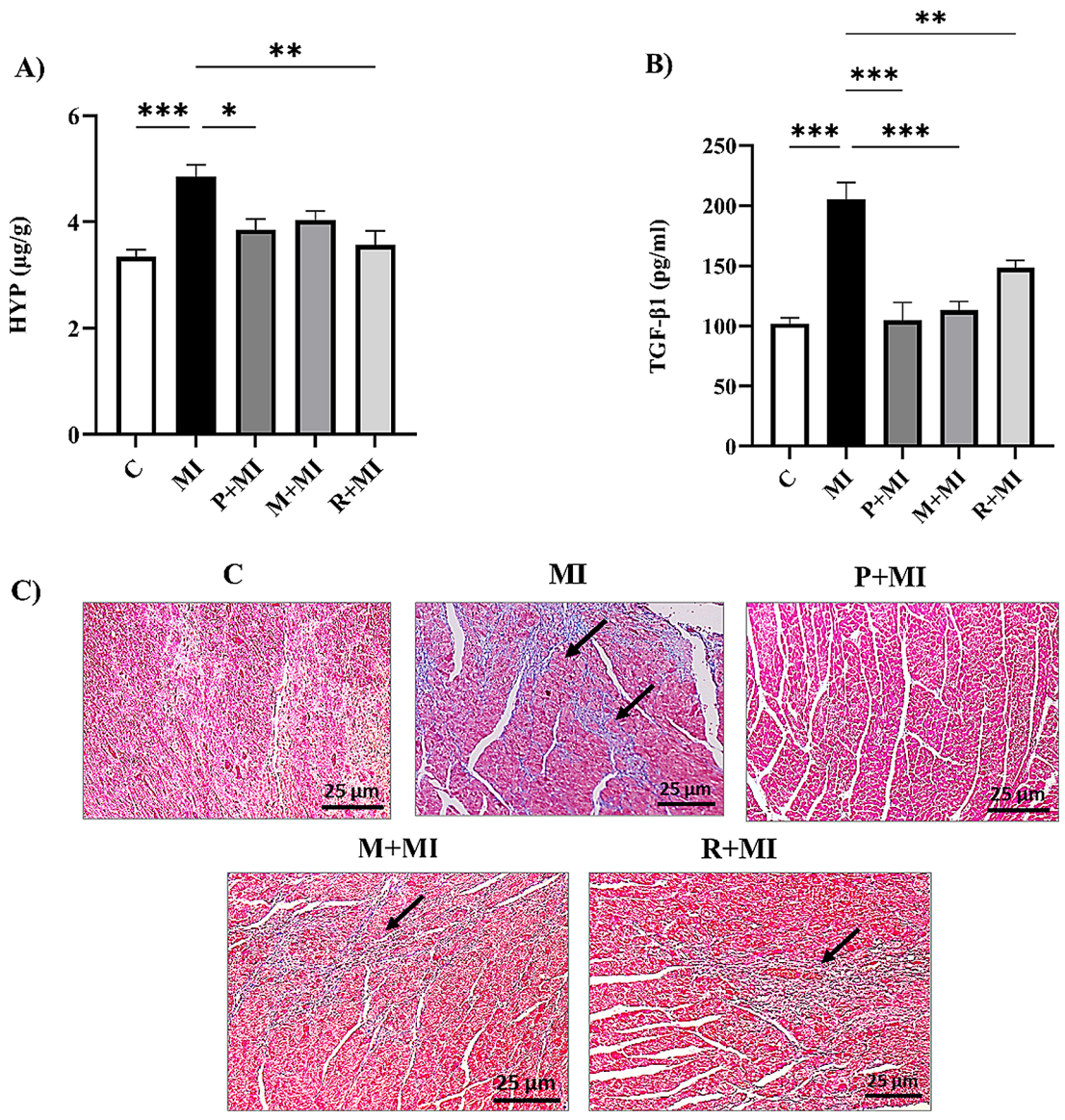

Fig. 4 Effects of paroxetine on heart fibrosis. HYP (**A**) and TGF-β1 (**B**) as indicators of cardiac fibrosis. **C** Cardiac muscle with Masson's trichrome staining: no fibrosis was seen in the normal control group, and moderate fibrosis (highlighted by blue stain) was seen in the MI group (20X power field). All data are expressed as means ± SEM of 6 animals per group. Differences between groups were determined using a one-way ANOVA followed by Dunnett's post hoc test. The total number of biological and technical replicates is 6 per group. Statistically significant changes compared to the untreated MI rats are indicated with * ($P < 0.05$), ** ($P < 0.01$), *** ($P < 0.001$). *Abbreviations C* control, *MI* untreated myocardial infarction, *P + MI* myocardial infarction pre-treated with paroxetine, *M + MI* myocardial infarction pre-treated with metoprolol, *R + MI* myocardial infarction pre-treated with irbesartan

As shown in Fig. 7A–C, antioxidant activity was inhibited significantly, including catalase ($P<0.01$), GSH ($P<0.01$), and SOD ($P<0.001$), in the MI group compared to the control rats. Pre-treatment with paroxetine increased antioxidant activity significantly, including GSH ($P<0.01$) and SOD ($P<0.001$), compared to the rats with untreated MI. Similarly, pre-treatment with either metoprolol or irbesartan significantly restored the antioxidant activity levels. On the other hand, the LPO levels and total nitrite (Fig. 7D–E) increased significantly in the MI group ($P<0.001$) compared with the control group. Pre-treatment with paroxetine, metoprolol, or irbesartan significantly decreased LPO and total nitrite ($P<0.001$) compared to the untreated MI group.

Discussion

GRK2 upregulation is linked to the progression of cardiovascular diseases. Enhanced GRK2 levels could be involved in post-MI cardiac remodeling [14, 38]. In the current study, paroxetine inhibited GRK2 activity, representing a significant advance in cardiovascular research. Paroxetine is an FDA-approved SSRI and has been shown to inhibit GRK2 activation in previous studies [21]. Published reports suggest that paroxetine

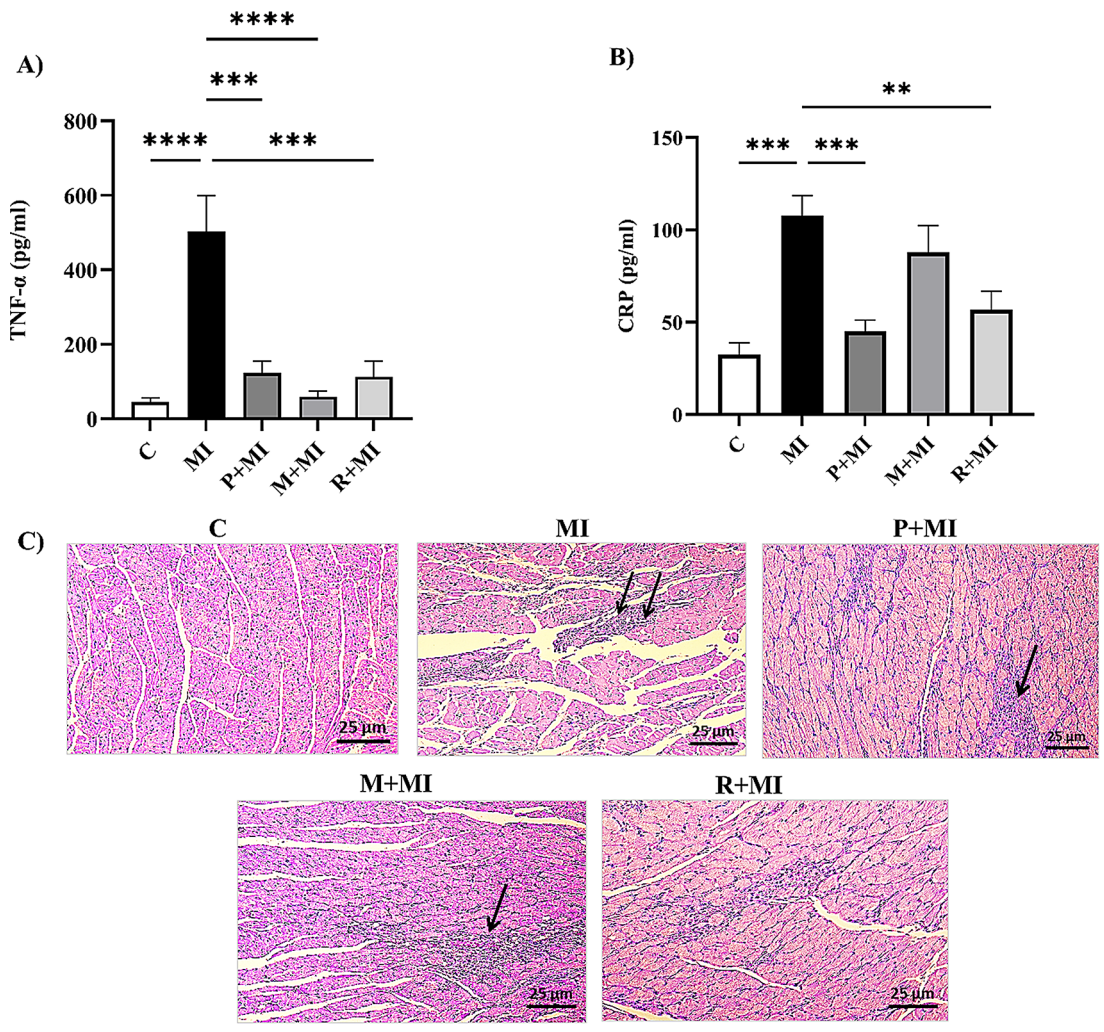

Fig. 5 Effects of paroxetine on inflammation. TNF-α (**A**) and serum level of CRP (**B**) for evaluation of inflammation. **C** PAS-stained cardiac tissue sections show positive macrophages (black arrows) (20X power field). All data are expressed as means ± SEM. Differences between groups were determined using one-way ANOVA followed by Dunnett's post hoc test. The total number of biological and technical replicates is 6 per group. Statistically significant changes compared to untreated MI rats are indicated with ** ($P < 0.01$), *** ($P < 0.001$), or **** ($P < 0.0001$). *Abbreviations C* control, *MI* untreated myocardial infarction, *P + MI* myocardial infarction pre-treated with paroxetine, *M + MI* myocardial infarction pre-treated with metoprolol, *R + MI* myocardial infarction pre-treated with irbesartan

might have a cardioprotective effect. However, its protective effect on MI-induced cardiac remodeling has yet to be elucidated. Thus, the current study was conducted to determine the potential protective effect of paroxetine, as a GRK2 inhibitor, on the progression of MI-associated remodeling. Furthermore, its effect was compared to those of a β-blocker and an AT1 receptor antagonist. The current findings suggest that pre-treatment with paroxetine may exert a beneficial effect that protects against post-MI cardiac remodeling, including modulating fibrosis, inflammation, and angiogenesis-related factors, similar to the effects of β-blockers and AT1 receptor antagonists (Table 1). This suggests a possible role for paroxetine as a cardioprotective treatment that attenuates the remodeling processes induced by myocardial infarction.

The current study used ISO to induce MI in an animal model. This model is commonly used to induce MI in animals and to investigate post-MI cardiac remodeling [8]. Various parameters confirmed MI induction. Firstly, the HW/BW ratio was increased in ISO-treated rats (MI). Additionally, the histopathological investigation showed morphological changes and increased serum levels of cTn-I, CK-MB, and LDH, confirming MI induction. These findings are consistent with those of previous studies, which found that cardiac injury biomarkers increased due to ISO-induced MI [39, 40].

Paroxetine was found to decrease the HW/BW ratio, cardiac troponin, and CK-MB, in agreement with previous studies showing that paroxetine treatment reduced heart enlargement (lower HW/BW ratio) and markers of cardiac injury (troponin and CK-MB levels) due to

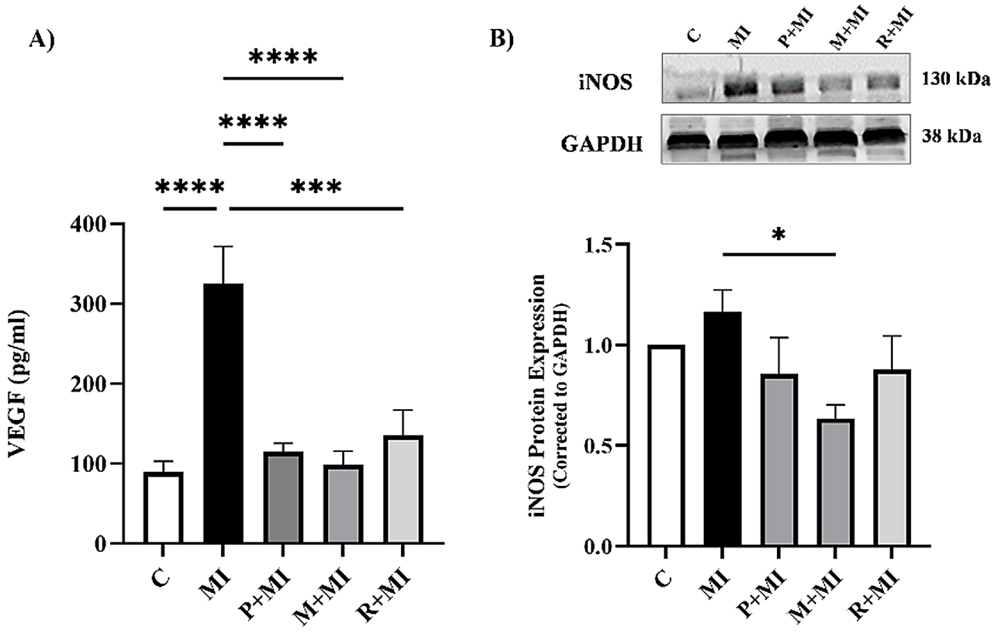

Fig. 6 Effect of paroxetine on VEGF and iNOS expression. The VEGF (**A**) and iNOS protein levels (**B**) (upper panel) and a representative immunoblot of the iNOS protein levels in the tissue homogenates of the left ventricle (lower panel) show the quantitative results of the immunoblot analysis. The iNOS protein expression was normalized to GAPDH, and the band densities were quantified using ImageJ software. The relative quantities are expressed in terms of the induced fold change. All data are expressed as means ± SEM ($n = 4$). Differences between groups were determined using a one-way ANOVA followed by Dunnett's post hoc test. Statistically significant changes compared to the untreated MI rats are indicated with * ($P < 0.05$), *** ($P < 0.001$), or **** ($P < 0.0001$). *Abbreviations C* control, *MI* untreated myocardial infarction, *P + MI* myocardial infarction pre-treated with paroxetine, *M + MI* myocardial infarction pre-treated with metoprolol, *R + MI* myocardial infarction pre-treated with irbesartan

hypertension-induced hypertrophy and ISO-induced MI, respectively [30]. Additionally, to the best of our knowledge, no studies have investigated the effects of paroxetine on LDH levels in CVDs. FGF23 is a crucial regulator of mineral metabolism that is known to be associated with myocardial remodeling, including the development of left ventricular (LV) hypertrophy and myocardial fibrosis [41].

Our findings show that FGF23 was slightly increased in rats with MI, confirming cardiac remodeling, which was consistent with previous reports that demonstrated a positive correlation between FGF23 and MI [42, 43]. Remarkably, we observed that pre-treatment with paroxetine attenuated the FGF23 levels, suggesting a potential protective effect against cardiac remodeling. To the best of our knowledge, no published study has investigated the effect of paroxetine on the MI-induced increase in the circulatory level of FGF23. Moreover, our findings show that treatment with metoprolol or irbesartan decreased plasma FGF23 levels. This outcome was consistent with those of previous studies, which showed that the use of β-adrenergic blockers or AT1 receptor antagonists decreased FGF23 levels [44, 45].

Post-MI fibrosis was evaluated by examining hydroxyproline, TGF-β1, and collagen deposition via Masson trichome staining. Hydroxyproline, a component of collagen, has been widely used as a marker of fibrosis in various studies investigating MI and related cardiac conditions [46, 47]. In the context of ISO-induced MI in rats, it has been observed that the TGF-β1 and hydroxyproline contents in rat hearts increase significantly, indicating increased collagen deposition and fibrosis [34, 48]. Pre-treatment with paroxetine results in a reduction in hydroxyproline levels, as evidenced by our investigation. This result aligns with an existing study showing that a paroxetine treatment reduced hydroxyproline levels, indicating potential reductions in collagen deposition and fibrosis in the heart [24]. Our investigation demonstrated that pre-treatment with metoprolol or irbesartan resulted in consistent reductions in hydroxyproline levels. We noticed similarities between our findings and a previous report, where metoprolol and carvedilol reduced the hydroxyproline content and the myocardial interstitial collagen volume fraction (ICVF) in a rat model of MI [49]. Further, a study investigating irbesartan effects on myocardial fibrosis in rats with diabetic cardiomyopathy demonstrated a decrease in the hydroxyproline level, suggesting a reduction in fibrosis [50]. These reports support our findings of pharmacological administration of both AT-1 and beta blockers.

The TNF-α is a key inflammatory marker that is closely associated with MI. TNF-α contributes to the injury processes and is mainly involved in the inflammatory phase of ventricular remodeling after MI [51]. In our results,

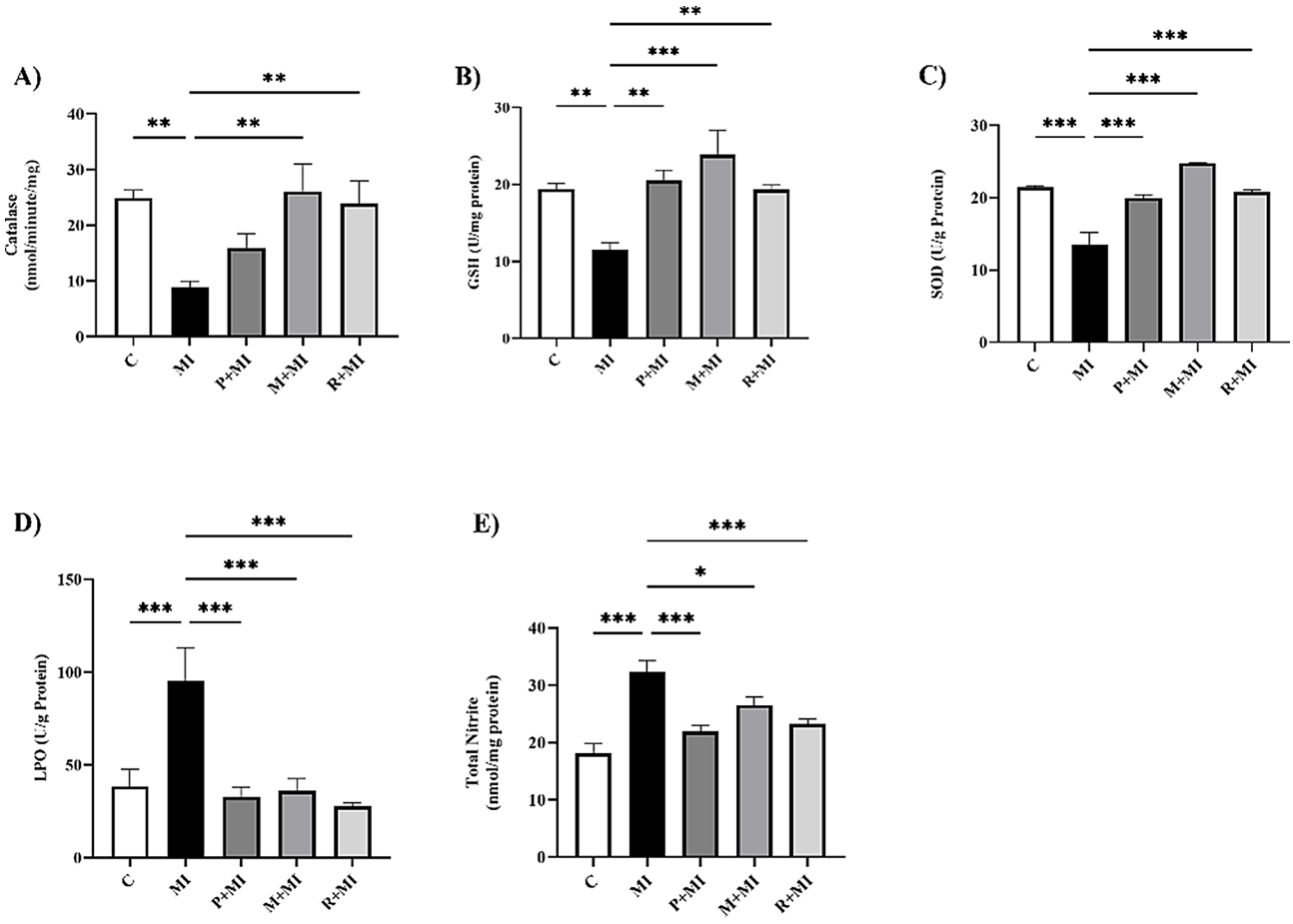

Fig. 7 Effects of paroxetine on oxidative stress biomarkers. Effects of paroxetine on catalase (**A**), GSH (**B**), SOD (**C**), LPO (**D**), and total nitrate (**E**) in cardiac tissue. All data are expressed as means ± SEM. Differences between groups were determined using one-way ANOVA followed by Dunnett's post hoc test. The total number of biological replicates is 6 per group. Statistically significant changes compared to untreated MI rats are indicated with * ($P < 0.05$), ** ($P < 0.01$), *** ($P < 0.001$). *Abbreviations C* control, *MI* untreated myocardial infarction, *P + MI* myocardial infarction pre-treated with paroxetine, *M + MI* myocardial infarction pre-treated with metoprolol, *R + MI* myocardial infarction pre-treated with irbesartan

the rats with MI exhibited increased TNF-α levels, consistent with previous reports that linked inflammatory responses to post-MI [52–54]. Pre-treatment with paroxetine reduced the TNF-α level, which was consistent with previous reports that showed the relationship between paroxetine and inflammatory markers and indicated that paroxetine has anti-inflammatory properties [55, 56]. Our findings suggest that pre-treatment with either metoprolol or irbesartan reduced TNF-α in rats with MI. The effects of metoprolol and irbesartan on TNF-α levels have been studied in animal models of MI. Early treatment with metoprolol has been shown to reduce TNF-α levels and can potentially mitigate MI by enhancing heart function and modulating the production of inflammatory cytokines. Irbesartan has been shown to reduce TNF-α and improve cardiac function in animal models of MI [57, 58].

Moreover, paroxetine pre-treatment attenuated CRP, which was consistent with previous studies reporting that paroxetine affects CRP serum levels in depressed patients [59]. CRP was also attenuated by β-blockers, in agreement with Yuji et al. (2007), who showed that a β-blocker treatment was associated with reducing an inflammatory marker in certain patients with congestive heart failure [60].

VEGF is an important marker of angiogenesis, which plays a crucial role in the context of MI [61]. A previous study showed that VEGF-A levels peaked within the first 24 h after MI, indicating a transient response that was crucial for initiating angiogenesis. Increased expression of VEGFRs was observed in the border zone, suggesting their involvement in mediating the pro-angiogenic effects of VEGF-A. Another study successfully used positron emission tomography (PET) imaging to confirm the presence of VEGFRs in the hearts of rats after MI. They developed a specific tracer, 64Cu-DOTA-VEGF121, that binds to VEGFRs [62, 63]. These two studies were consistent with our findings regarding the elevation of VEGF in rats with MI. Our study demonstrated that pre-treatment with paroxetine reduced the VEGF levels in rats with MI.

Table 1 Comparative summary of the effects of paroxetine, metoprolol, and irbesartan on post-MI cardiac remodeling in ISO-induced cardiac injury animal model

Groups (pre-treatment)	Paroxetine	Metoprolol	Irbesartan
HW/BW ratio	**	***	***
cTn-I	***	***	***
CK-MB	***	***	**
LDH	n/s	*	**
FGF23	**	n/s	n/s
HYP	*	n/s	**
TGF-β1	***	***	**
TNF-α	***	***	***
CRP	***	n/s	**
Catalase	n/s	**	**
GSH	**	***	**
SOD	***	***	***
LPO	***	***	***
Total Nitrite	***	*	***

Note (*) represent differences in comparison to MI-untreated rats, were * ($P<0.05$), ** ($P<0.01$), *** ($P<0.001$)

Abbreviations HW/BW ratio heart weight/body weight ratio, *cTn-I* cardiac troponin I, *CK-MB* creatine kinase myocardial band, *LDH* lactate dehydrogenase, *FGF23* fibroblast growth factor 23, *HYP* hydroxyproline, *TGF-β1* transforming growth factor-β1, *TNF-α* tumor necrosis factor α, *CRP* C reactive protein, *GSH* Glutathione Reductase, *LPO* lipid peroxidation, *SOD* Superoxide dismutase

This finding suggests a potential role for paroxetine in modulating post-MI angiogenesis.

A limited body of research currently investigates the interaction between paroxetine and VEGF in the context of MI. Notably, a single study found that four weeks of paroxetine treatment in patients with major depression did not alter plasma VEGF levels. Additionally, no correlation was observed between changes in VEGF and the clinical response to paroxetine [64]. In contrast, our findings suggest that pre-treatment with metoprolol decreased VEGF levels. On the other hand, a previous study demonstrated that carvedilol, a beta-blocker used in patients with chronic heart failure, led to increased plasma VEGF levels [65]. Besides, another study demonstrated that metoprolol, when employed as a therapeutic agent, did not significantly influence the VEGF levels within the ischemic myocardium in a rat model [66]; these controversial effects could be driven by the fact that beta-blocker cardioprotective modulations could be affected by disease-based pathological mechanism.

Our investigation revealed that irbesartan reduced the VEGF levels in our rat model of MI. This finding aligns with a previous report demonstrating irbesartan's ability to decrease VEGF expression in response to lipopolysaccharide (LPS)-induced cardiotoxicity. In that study, LPS exposure elevated VEGF levels in both the heart and aorta, while irbesartan treatment reversed this increase [67]. Cardiac myocytes have been shown to produce iNOS, and this expression is augmented in the myocardium of failing hearts and results in increased circulating NO levels [68]. Even though increased NO production from iNOS may have a beneficial effect via reducing vascular resistance, high levels of NO production might reduce the contractility of the myocardium and may produce myocardial damage [69]. Furthermore, enhanced NO production due to iNOS expression contributes to myocardial dysfunction and mortality after infarction in a mouse model of MI [70]. This is consistent with the findings of the current study, where the iNOS protein level was enhanced after MI.

Other important markers of post-MI injury include oxidative stress markers and antioxidants such as catalase, GSH, and SOD, which limit ROS production and protect damaged cellular components [71]. Our investigation revealed that the levels of these antioxidants were reduced in rats with untreated myocardial infarctions, which agrees with a previous study [72]. Similarly, Aladag et al. (2021) reported that catalase and SOD were reduced in a patient with a myocardial infarction [73]. In terms of the effect of paroxetine, the current findings show that pre-treatment with paroxetine restores the antioxidant activity of catalase, SOD, and GSH. Moreover, it attenuates the LPO and total nitrate levels. In agreement with our findings, Lassen et al. (2017) reported that paroxetine treatment reduced ROS production in the myocardium within the first week after MI and eventually reduced left ventricular remodeling following MI [74]. Further investigations could be conducted as future directions such as verify these findings by examining the biomarkers at the mRNA level, investigation them on clinical levels, also validate them by utilizing another model of MI such as ligation induced infraction.

Collectively, these evaluations of the main endpoints for fibrosis, inflammation, oxidative stress, and angiogenesis, as well as histological and morphological changes, reveal significant insights into therapeutic impacts across different experimental treatments, highlighting the nuanced effects of various treatments on the progression of post-MI remodeling in cardiac muscle in rats. In conclusion, we have shown that pre-treatment with paroxetine protects the myocardium during the early stage of pathological cardiac remodeling. Furthermore, we observed effects similar to those observed with β-blockers or angiotensin receptor antagonists. However, clinical studies of paroxetine must be carried out to determine whether GRK2 inhibition can prevent post-MI cardiac remodeling. Compared to β-blockers, the additive beneficial effect of paroxetine in the standard therapy, which includes β-blockers, is expected to be limited. On the other hand, paroxetine becomes particularly promising when a patient requires an SSRI to treat another disease or when other medications, such as β-blockers or angiotensin receptor antagonists, are not tolerated or recommended. Further studies are needed to

investigate the effect of paroxetine-mediated GRK2 inhibition on possible GRK2-mediated molecular signaling mechanisms in cardiac remodeling processes.

Abbreviations

CRP	C-reactive protein
CK-MB	Creatine kinase MB
ELISA	Enzyme-linked immunosorbent assay
FGF23	Fibroblast growth factor 23
GSH	Glutathione Reductase
GPCR	G-protein coupled receptor
GRK2	G protein-coupled receptor kinase 2
GAPDH	Glyceraldehyde 3-phosphate dehydrogenase
HYP	Hydroxyproline
ISO	Isoproterenol
IP	Intraperitoneal
LDH	Lactate dehydrogenase
LPO	Lipid peroxidation
MI	Myocardial infarction
MT	Masson trichrome stain
Tn-I	Troponin 1
TGF-β1	Transforming growth factor-β1
TNFα	Tumor necrosis factor-α
SOD	Superoxide dismutase
SSRI	Selective Serotonin Reuptake Inhibitor

Supplementary Information

The online version contains supplementary material available at https://doi.org/10.1186/s40360-024-00824-9.

Supplementary Material 1

Acknowledgements
The authors extend their appreciation to the Deputyship for Research and Innovation of the "Ministry of Education" in Saudi Arabia for funding this research work through project IFKSUDR_H150.

Author contributions
Conceptualization, Anfal Bin Dayel; Formal analysis, Maha Alamin; Funding acquisition, Asma Alonazi; Investigation, Sara Almodawah, Rana Aldigi, Maha Alamin, Ahmad Almotairi, Maha EL-Tohamy and Hana Alharbi; Methodology, Sara Almodawah, Rana Aldigi, Maha Alamin, Ahmad Almotairi, Maha EL-Tohamy and Rehab Ali; Project administration, Asma Alonazi and Anfal Bin Dayel; Resources, Asma Alonazi; Software, Sara Almodawah, Rana Aldigi, Maha Alamin and Ahmad Almotairi; Supervision, Asma Alonazi; Writing – original draft, Sara Almodawah and Rana Aldigi; Writing – review & editing, Asma Alonazi, Anfal Bin Dayel, Tahani Alshammari and Nouf Alrasheed.

Funding
The authors extend their appreciation to the Deputyship for Research and Innovation of the "Ministry of Education" in Saudi Arabia for funding this research work through project IFKSUDR_H150.

Data availability
No datasets were generated or analysed during the current study.

Declarations

Ethical approval
The animal study protocol was reviewed and approved by the Ethics Committee of King Saud University (Reference: KSU-SE-23-41, issued on 16th May 2023).

Informed consent
Not applicable, as the current study did not involve humans.

Competing interests
The authors declare no competing interests.

Received: 20 July 2024 / Accepted: 10 December 2024
Published online: 18 December 2024

References

1. World Health Organization. Cardiovascular diseases. Accessed 14 Apr 2023.
2. Khan MA, et al. Global Epidemiology of Ischemic Heart Disease: Results from the Global Burden of Disease Study. Cureus. 2020;12(7):e9349.
3. Pereira E, Pereira H. Socioeconomic impact of cardiovascular disease. Rev Port Cardiol (Engl Ed). 2020;39(5):253–4.
4. Frangogiannis NG. Pathophysiology of Myocardial Infarction. Compr Physiol. 2015;5(4):1841–75.
5. Aydin S, et al. Biomarkers in acute myocardial infarction: current perspectives. Vasc Health Risk Manag. 2019;15:1–10.
6. Frangogiannis NG. The inflammatory response in myocardial injury, repair, and remodelling. Nat Rev Cardiol. 2014;11(5):255–65.
7. Zhang RYK, et al. Impact of Reperfusion on Temporal Immune Cell Dynamics After Myocardial Infarction. J Am Heart Assoc. 2023;12(4):e027600.
8. Prabhu SD, Frangogiannis NG. The Biological Basis for Cardiac Repair After Myocardial Infarction: From Inflammation to Fibrosis. Circ Res. 2016;119(1):91–112.
9. Shibuya M. Vascular Endothelial Growth Factor (VEGF) and Its Receptor (VEGFR) Signaling in Angiogenesis: A Crucial Target for Anti- and Pro-Angiogenic Therapies. Genes Cancer. 2011;2(12):1097–105.
10. Cohn JN, Ferrari R, Sharpe N. Cardiac remodeling–concepts and clinical implications: a consensus paper from an international forum on cardiac remodeling. Behalf of an International Forum on Cardiac Remodeling. J Am Coll Cardiol. 2000;35(3):569–82.
11. Lai S, et al. G protein-coupled receptor kinase-2: A potential biomarker for early diabetic cardiomyopathy. J Diabetes. 2020;12(3):247–58.
12. Vasudevan NT, et al. Regulation of β-adrenergic receptor function: an emphasis on receptor resensitization. Cell Cycle. 2011;10(21):3684–91.
13. Belmonte SL, Blaxall BC. G protein coupled receptor kinases as therapeutic targets in cardiovascular disease. Circ Res. 2011;109(3):309–19.
14. Murga C, et al. Protein-Coupled Receptor Kinase 2 (GRK2) as a Potential Therapeutic Target in Cardiovascular and Metabolic Diseases. Front Pharmacol. 2019;10:112.
15. Cannavo A, Liccardo D, Koch WJ. Targeting cardiac β-adrenergic signaling via GRK2 inhibition for heart failure therapy. Front Physiol. 2013;4:264.
16. Arcones AC, et al. G protein–coupled receptor kinase 2 at crossroads of metabolic and cardiovascular diseases. Curr Opin Endocr Metabolic Res. 2021;16:75–85.
17. Iaccarino G, et al. Elevated myocardial and lymphocyte GRK2 expression and activity in human heart failure. Eur Heart J. 2005;26(17):1752–8.
18. Bourin M, Chue P, Guillon Y. Paroxetine: a review. CNS Drug Rev. 2001;7(1):25–47.
19. Thal DM, et al. Paroxetine is a direct inhibitor of g protein-coupled receptor kinase 2 and increases myocardial contractility. ACS Chem Biol. 2012;7(11):1830–9.
20. Guo S, Carter R, Tilley D. Impact of paroxetine on proximal β-adrenergic receptor signaling. FASEB J. 2017;31(S1):992.3-992.3.
21. Schumacher SM, et al. Paroxetine-mediated GRK2 inhibition reverses cardiac dysfunction and remodeling after myocardial infarction. Sci Transl Med. 2015;7(277):277ra31.
22. Xu H, et al. Paroxetine and Mortality in Heart Failure: A Retrospective Cohort Study. Front Cardiovasc Med. 2021;8:794584.
23. Yeragani VK, et al. Major depression with ischemic heart disease: effects of paroxetine and nortriptyline on long-term heart rate variability measures. Biol Psychiatry. 2002;52(5):418–29.
24. Alonazi AS, et al. Cardioprotective effects of the GRK2 inhibitor paroxetine on isoproterenol-induced cardiac remodeling by modulating NF-κB mediated prohypertrophic and profibrotic gene expression. Int J Mol Sci. 2023;24(24):17270.
25. Won H, et al. Clinical Impact of Beta Blockers in Patients with Myocardial Infarction from the Korean National Health Insurance Database. Korean Circ J. 2020;50(6):499–508.

26. Hanatani A, et al. Inhibition by angiotensin II type 1 receptor antagonist of cardiac phenotypic modulation after myocardial infarction. J Mol Cell Cardiol. 1995;27(9):1905–14.
27. Azevedo PS, et al. Cardiac remodeling: concepts, clinical impact, pathophysiological mechanisms and pharmacologic treatment. Arq Bras Cardiol. 2016;106(1):62–9.
28. Lobo Filho HG, et al. Experimental model of myocardial infarction induced by isoproterenol in rats. Rev Bras Cir Cardiovasc. 2011;26(3):469–76.
29. Mnafgui K, et al. Protective Effect of Hydroxytyrosol Against Cardiac Remodeling After Isoproterenol-Induced Myocardial Infarction in Rat. Cardiovasc Toxicol. 2016;16(2):147–55.
30. Sun X, et al. Paroxetine Attenuates Cardiac Hypertrophy Via Blocking GRK2 and ADRB1 Interaction in Hypertension. J Am Heart Association. 2021;10(1):e016364.
31. Qin W, et al. Metoprolol protects against myocardial infarction by inhibiting miR-1 expression in rats. J Pharm Pharmacol. 2020;72(1):76–83.
32. Leenen FH, Yuan B. Prevention of hypertension by irbesartan in Dahl S rats relates to central angiotensin II type 1 receptor blockade. Hypertension. 2001;37(3):981–4.
33. Shi H, et al. The Effect of Electronic-Cigarette Vaping on Cardiac Function and Angiogenesis in Mice. Sci Rep. 2019;9(1):4085.
34. Wang QW, et al. Ginsenoside Re Improves Isoproterenol-Induced Myocardial Fibrosis and Heart Failure in Rats. Evid Based Complement Alternat Med. 2019;2019:3714508.
35. Moron MS, Depierre JW, Mannervik B. Levels of glutathione, glutathione reductase and glutathione S-transferase activities in rat lung and liver. Biochim Biophys Acta. 1979;582(1):67–78.
36. Delides A, et al. An optimized semi-automatic rate method for serum glutathione reductase activity and its application to patients with malignant disease. J Clin Pathol. 1976;29(1):73–7.
37. Ohkawa H, Ohishi N, Yagi K. Assay for lipid peroxides in animal tissues by thiobarbituric acid reaction. Anal Biochem. 1979;95(2):351–8.
38. Huang ZM, et al. GRK2 in the heart: a GPCR kinase and beyond. Antioxid Redox Signal. 2014;21(14):2032–43.
39. Chen W, et al. Cardioprotection of cortistatin against isoproterenol-induced myocardial injury in rats. Ann Transl Med. 2020;8(6):309.
40. Ahmed MI, et al. Cardioprotective effect of flibanserin against isoproterenol-induced myocardial infarction in female rats: role of cardiac 5-HT2A receptor gene/5-HT/Ca(2+) pathway. Pharmaceuticals (Basel). 2023;16(4):502.
41. Cornelissen A, et al. Fibroblast growth factor 23 and outcome prediction in patients with acute myocardial infarction. J Clin Med. 2022;11(3):601.
42. Stöhr R, et al. FGF23 in cardiovascular disease: innocent bystander or active mediator? Front Endocrinol. 2018;9:351.
43. Thorsen IS, et al. The relationship between Fibroblast Growth Factor 23 (FGF23) and cardiac MRI findings following primary PCI in patients with acute first time STEMI. Int J Cardiol Heart Vasc. 2021;33:100727.
44. Tsai CK, et al. Low-dose propranolol prevents functional decline in catecholamine-induced acute heart failure in rats. Toxics. 2022;10(5):238.
45. Böckmann I, et al. FGF23-mediated activation of local RAAS promotes cardiac hypertrophy and fibrosis. Int J Mol Sci. 2019;20(18):4634.
46. Meng Q, et al. MMI-0100 inhibits cardiac fibrosis in a mouse model overexpressing cardiac myosin binding protein C. J Am Heart Assoc. 2017;6(9):e006590.
47. Wynn TA. Cellular and molecular mechanisms of fibrosis. J Pathol. 2008;214(2):199–210.
48. Wang F, et al. Apigenin inhibits isoproterenol-induced myocardial fibrosis and Smad pathway in mice by regulating oxidative stress and miR-122-5p/155-5p expressions. Drug Dev Res. 2022;83(4):1003–1015.
49. Sun T, et al. [Effects of carvedilol and metoprolol on cardiac fibrosis in rats with experimental myocardial infarction]. Zhonghua xin xue guan bing za zhi. 2008;36(1):68–71.
50. Zong M, et al. Irbesartan ameliorates myocardial fibrosis in diabetic cardiomyopathy rats by inhibiting the TGFβ1/Smad2/3 pathway. Exp Ther Med. 2020;20(5):117.
51. Tian M, et al. Tumor necrosis factor-α and its role as a mediator in myocardial infarction: A brief review. Chronic Dis Transl Med. 2015;1(1):18–26.
52. Irwin MW, et al. Tissue expression and immunolocalization of tumor necrosis factor-alpha in postinfarction dysfunctional myocardium. Circulation. 1999;99(11):1492–8.
53. Mahmoud AH, et al. PTEN gene & TNF-alpha in acute myocardial infarction. Int J Cardiol Heart Vasc. 2019;23:100366.
54. Ibarra-Lara MdlL, et al. Peroxisome proliferator-activated receptors (PPAR) downregulate the expression of pro-inflammatory molecules in an experimental model of myocardial infarction. Can J Physiol Pharmacol. 2016;94(6):634–42.
55. Durairaj H, Steury MD, Parameswaran N. Paroxetine differentially modulates LPS-induced TNFα and IL-6 production in mouse macrophages. Int Immunopharmacol. 2015;25(2):485–92.
56. Kabiri M, et al. Paroxetine modulates immune responses by activating a JAK2/STAT3 signaling pathway. J Biochem Mol Toxicol. 2020;34(5):e22464.
57. Berthonneche C, et al. AT1 receptor blockade prevents cardiac dysfunction after myocardial infarction in rats. Cardiovasc Drugs Ther. 2005;19(4):251–9.
58. Boccellino M, et al. AT1-receptor blockade: Protective effects of irbesartan in cardiomyocytes under hypoxic stress. PLoS ONE. 2018;13(10):e0202297.
59. Carboni L, et al. Biomarkers for response in major depression: comparing paroxetine and venlafaxine from two randomised placebo-controlled clinical studies. Transl Psychiatry. 2019;9(1):182.
60. Nagatomo Y, et al. Effects of beta-blocker therapy on high sensitivity c-reactive protein, oxidative stress, and cardiac function in patients with congestive heart failure. J Card Fail. 2007;13(5):365–71.
61. Zhou Y, et al. The Role of the VEGF Family in Coronary Heart Disease. Front Cardiovasc Med. 2021;8:738325.
62. Rodriguez-Porcel M, et al. Imaging of VEGF receptor in a rat myocardial infarction model using PET. J Nucl Med. 2008;49(4):667–73.
63. Zhao T, et al. Vascular endothelial growth factor (VEGF)-A: role on cardiac angiogenesis following myocardial infarction. Microvasc Res. 2010;80(2):188–94.
64. Yoshimura R, Okamoto N, Ikenouchi A. Effects of Paroxetine on Plasma Levels of Vascular Endothelial Growth Factor in Patients with Major Depression. Psychiatr Danub. 2022;34(3):533–4.
65. de Boer RA, et al. Carvedilol increases plasma vascular endothelial growth factor (VEGF) in patients with chronic heart failure. Eur J Heart Fail. 2001;3(3):331–3.
66. Fan Y, et al. Effects of metoprolol on serum inflammatory factors and myocardial ischemia in rats modeled with coronary heart disease. Am J Transl Res. 2021;13(4):2518–27.
67. Tepebaşi MY, et al. Irbesartan has a curative effect on lipopolysaccharide-induced cardiotoxicity by antioxidant and antiapoptotic pathways. Rev Port Cardiol. 2023;42(11):895–903.
68. Vejlstrup NG, et al. Inducible nitric oxide synthase (iNOS) in the human heart: expression and localization in congestive heart failure. J Mol Cell Cardiol. 1998;30(6):1215–23.
69. Ferdinandy P, et al. Peroxynitrite is a major contributor to cytokine-induced myocardial contractile failure. Circ Res. 2000;87(3):241–7.
70. Feng Q, et al. Increased Inducible Nitric Oxide Synthase Expression Contributes to Myocardial Dysfunction and Higher Mortality After Myocardial Infarction in Mice. Circulation. 2001;104(6):700–4.
71. Panda P, et al. Biomarkers of Oxidative Stress Tethered to Cardiovascular Diseases. Oxid Med Cell Longev. 2022;2022:p9154295.
72. Abbas AM. Cardioprotective effect of resveratrol analogue isorhapontigenin versus omega-3 fatty acids in isoproterenol-induced myocardial infarction in rats. J Physiol Biochem. 2016;72(3):469–84.
73. Aladağ N, et al. Oxidants and antioxidants in myocardial infarction (MI): Investigation of ischemia modified albumin, malondialdehyde, superoxide dismutase and catalase in individuals diagnosed with ST elevated myocardial infarction (STEMI) and non-STEMI (NSTEMI). J Med Biochem. 2021;40(3):286–94.
74. Lassen TR, et al. Effect of paroxetine on left ventricular remodeling in an in vivo rat model of myocardial infarction. Basic Res Cardiol. 2017;112(3):26.

Publisher's note

Springer Nature remains neutral with regard to jurisdictional claims in published maps and institutional affiliations.